Energy &
Environmental Science

Dynamic Article Links

Cite this: *Energy Environ. Sci.*, 2012, **5**, 6188

www.rsc.org/ees

PAPER

Charge accumulation and electron transfer kinetics in *Geobacter sulfurreducens* biofilms†

Pablo Sebastián Bonanni, German D. Schrott, Luciana Robuschi and Juan Pablo Busalmen*

Received 14th September 2011, Accepted 6th January 2012
DOI: 10.1039/c2ee02672d

Electroactive bacteria can use a polarized electrode as final electron acceptor, allowing the use of electrochemical techniques for a very accurate quantification of its respiration rate. Biofilm cell respiration has been recently demonstrated to continue after the interruption of electrode polarization since these bacteria can store electrons in the haem groups of exocytoplasmic cytochromes. Interestingly, it has been shown that when the electrode is connected again, stored electrons can be recovered as a current superimposed to the basal steady state current produced by biofilm respiration. This work presents a model for the biofilm-catalysed electron transfer mechanism that reproduces the current profile obtained upon electrode reconnection. The model allows the estimation of kinetic parameters for internalization of the reduced substrate by the cells and the subsequent reduction of cell internal cytochromes, the electron transfer to mediators in the exterior of the cell, charge transport across the biofilm matrix to the electrode through fixed mediators and, finally, the oxidation of cytochromes at the biofilm/electrode interface. Based on these estimates, the distribution of stored charge within the biofilm can also be calculated. The results indicate that the processes involved in electron transfer from acetate to internal cytochromes represent the main limitation to current production, showing that both electron transport through the matrix of cytochromes and interfacial electron transfer are orders of magnitude faster than this process. Stored charge, on the other hand, is an order of magnitude higher inside the cells compared with that in the conductive matrix, suggesting that internal cytochromes are approximately ten times more abundant inside the cells than in the conductive matrix.

Introduction

Understanding the extracellular electron transport mechanisms in electricity-producing biofilms and the factors controlling the rate and extent of the process is important for the optimization of practical applications and a better modeling of natural and/or industrial systems.[1,2] A complete description of the electron transport mechanisms in electricity-producing biofilms has not yet been achieved, but two main types, direct and mediated by soluble electron shuttles, can be distinguished.[2–5] In the case of *G. sulfurreducens*, electrochemical studies[6,7] have confirmed that electron transport to the electrode does not proceed through electron shuttles but through a direct physical connection *via* external c-type cytochromes.[2,3,8,9] It has been also shown that high current densities in biofilms of this strain can only be obtained if electron transport proceeds through a fixed conductive matrix[5,10,11] and recent work indicates that exopolysaccharides,[12] pili[13,14] and extracellular cytochromes such as

Laboratorio de Bioelectroquímica, División Corrosión, INTEMA (CONICET), Juan B. Justo 4302, B7608FDQ Mar del Plata, Argentina. E-mail: jbusalme@fi.mdp.edu.ar

† Electronic supplementary information (ESI) available. See DOI: 10.1039/c2ee02672d

Broader context

Take my breath away. By disconnecting the electrode, electro-active biofilms are forced to accumulate charge using cell internal and external cytochromes as temporary electron acceptors for its respiratory chain. The discharge current profile obtained when those electrons are transferred to the electrode contains valuable information about the electron transport process. Here we present a model that suitably reproduces this current profile allowing the determination of the rate constant for steps involved in the transport process as well as charge distribution within the biofilm. The identification of the limiting step for current production will hopefully help to achieve more efficient bioelectrogenic devices such as microbial fuel cells, microbial electrolysis cells or whole cell biosensors.

OmcS and OmcZ[6] are involved either in supporting the biofilm structure or in the electron transfer processes. Anyway, a consensus on the role that each of these species has on the electron transport mechanism of *Geobacter sulfurreducens* biofilms has not yet been achieved. Actually, two different mechanisms are being proposed for the electron transport from the cells to the electrode: the metallic-like conduction through pili to interfacial cytochromes that make the final transfer to the electrode,[15,16] and the transfer through a sequence of redox reactions between cytochromes that connect biofilm cells to the electrode.[6,17,18] The model presented in this work subscribes to the latter proposal.

Although electron transport mechanisms are poorly understood, it is important to determine kinetic parameters in order to understand and control the biocatalytic processes. This problem has been approached by developing a kinetic model that combines Michaelis–Menten, Monod and Nernst classical equations.[19] In this way the dependence of the biofilm overall catalytic activity on the electrode potential and substrate concentration has been established and the crucial role of biofilm conductivity in the production of current has been demonstrated.[20] In addition, relevant qualitative analyses have been made using cyclic voltammetry to estimate the rate-limiting steps in electron transport from the substrate to the electrode.[6,21] In spite of these efforts, numerical data for relative rates of electron transport steps are still lacking.

It has been recently demonstrated that *Geobacter* cells store electrons in extracytoplasmic cytochromes in the absence of an electron acceptor.[17,22] When the polarization of the electrode is interrupted, the use of the extracytoplasmic cytochromes as an electron sink allows the activity of the cells to continue for some time leading to a net accumulation of charge in the biofilm. If the electrode is connected again, a transient current related to biofilm discharge is observed. Additional work (Schrott *et al.* in preparation) has shown that the discharge characteristics change during biofilm growth, showing the appearance of a current minimum (Fig. 1), which is considered a consequence of the contribution of at least two processes, the re-oxidation of cytochromes reduced during polarization interruption and the release of electrons by cell metabolism.

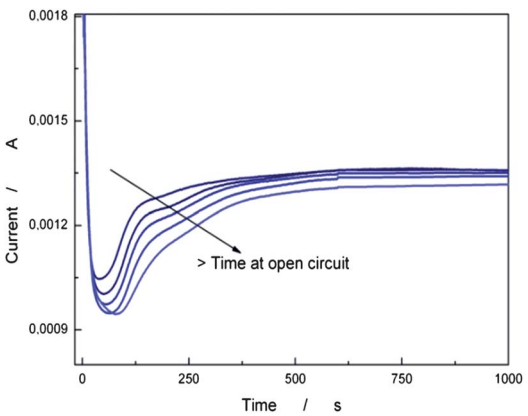

Fig. 1 Transient current obtained after connecting again the electrode for open circuit times of 10, 15, 20, 30 and 45 minutes. Applied potential = 0.4 V (SHE).

In order to reach the electrode, the charge stored in external cytochromes must be transported through the matrix to be subsequently transferred from the wiring cytochromes to the electrode in a very fast step.[6] The charge arising from central metabolic pathways, on the other hand, has to go through additional electron transfer steps in the respiratory chain reactions and transport through the periplasmic space before reaching the cell exterior. Indeed, the electron transfer from inside the cell requires a fraction of external cytochromes[17] in the oxidized form (with no stored charge) to act as electron acceptors and transporters, which clearly subordinates cell activity to the discharge of the matrix. Thus, it has been proposed that the current observed after connecting again the electrode will correspond initially to the discharge of the electrons accumulated in the biofilm cytochromes, while electrons from acetate oxidation will be collected later on.[17] In addition, as can be clearly seen in Fig. 1, the time needed for recovery of steady state current increases with the duration of the polarization interruption, suggesting that charge accumulation in the external network down regulates the contribution from the metabolic activity of cells.

The time evolution of the two contributions to the transient current (oxidation of the reduced cytochromes and metabolic activity) is also different. Similarly to the discharge of a capacitor, the rate of discharge of the electrons accumulated during the open circuit period will decrease progressively as the charge is transferred to the electrode, while the metabolic current will progress from zero (no activity in the cells) to a steady state value that will depend on the biofilm size and activity.

Based on the above interpretation, a new approach for the determination of electron transport kinetics in electricity-producing biofilms is presented in this work. By modeling the transient current obtained after polarization interruption and electrode re-connection, the rates of the steps involved in the electron transfer from the substrate to the electrode as well as charge distribution within the biofilm are estimated.

Based on previous works, the model considers a four-step mechanism to explain the electron transport rate from the

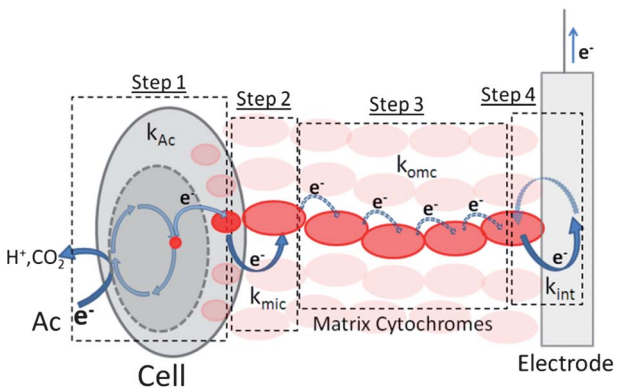

Fig. 2 Proposed steps for the electron transfer process in *Geobacter* biofilms. Step 1 represents acetate uptake and electron transfer to periplasmic (cell internal) cytochromes, step 2 the subsequent transfer to the exocytoplasmic (matrix) cytochromes, step 3 the transport along the biofilm matrix to the electrode interface and, finally, step 4 the heterogeneous transfer between the interfacial cytochromes and the electrode.

substrate to the electrode.[6,21] The proposed mechanism, shown schematically in Fig. 2, comprises: (1) substrate (acetate) uptake and electron transfer to cell internal cytochromes, (2) electron transfer to mediators in the cell exterior through the cell external membrane, (3) charge transport along the biofilm matrix to the biofilm/electrode interface through fixed mediators and (4) electron transfer to the electrode by oxidation of cytochromes at the biofilm/electrode interface.

It has to be noted that each of the mentioned steps may involve multiple reaction and transfer processes. For example, step 1, which accounts for acetate uptake and electron transfer to cell internal cytochromes, implicitly includes all the reactions of the citric acid cycle and also the electron transfer through the inner membrane. The kinetic constant of each step will be mainly determined by the rate of its limiting process.

Considering the proposed mechanism, when electrode polarization is interrupted the possible compartments where charge can be accumulated include the cytochromes at the periplasm (interior of the cell), those at the biofilm matrix, and the cytochromes situated at the biofilm–electrode interface. The amount of stored charge in each compartment at any given time after polarization interruption will depend on the total amount of cytochromes (external and internal), the duration of the interruption, the rate of substrate uptake and metabolization and the electron transfer rate between cytochromes.

In summary, to explain the transient current obtained after connecting again the electrode, two overlapping contributions with different rates are considered: the current produced by the discharge of accumulated electrons, decreasing over time in an exponential way (capacitor-like), and the current due to metabolic activity, increasing progressively to a steady state value. Once an expression for the transient current is found, it will be used to fit the experimental results in order to find the rate constant values for the steps involved in the electron transfer from the substrate to the electrode, as well as the charge distribution in the biofilm.

Derivation of the expression for the current transients

The mechanism considered for obtaining the time dependence of the current follows the scheme depicted in Fig. 2.[6] The biofilm is represented as a three-dimensional coating comprised of cells and cytochromes that act as bound electron transfer mediators. The mediators allow the transport of electrons from the cell to the electrode through the biofilm and across the biofilm/electrode interface. The electrochemical reactions taking place at each step are as follows:

$$\frac{1}{8}\,Ac^- + Mic_{ox} \xrightarrow{k_{Ac}} Mic_{red} + \frac{1}{4}CO_2 + H^+ \quad \text{Step 1}$$

$$Mic_{red} + Omc_{ox} \xrightarrow{k_{mic}} Mic_{ox} + Omc_{red} \quad \text{Step 2}$$

$$Omc_{red} + Omc^*_{ox} \xrightarrow{k_{omc}} Omc_{ox} + Omc^*_{red} \quad \text{Step 3}$$

$$Omc^*_{red} \xrightarrow{k_{int}} Omc^*_{ox} + e^- \quad \text{Step 4}$$

where Mic_{ox} represents haems of cell internal cytochromes, Omc_{ox} are the matrix cytochrome haems and Omc^*_{ox} are the interfacial cytochrome haems. The subscripts red and ox stand for the reduced and oxidized states. All four steps are considered to follow elementary kinetics. Mass transfer of the substrate to the biofilm is considered fast enough for being not rate limiting. This assumption is valid with proper stirring and for a bulk acetate concentration higher than 5 mM.[7] Step 1 should follow Michaelis–Menten kinetics[21] but under high acetate concentration its rate will depend only on the concentration of oxidized cells, Mic_{ox}. Step 4 is a fast redox process that can be described by the Butler–Volmer expressions for electrode reaction rates;[23] but at a sufficiently high anodic potential the reverse reaction can be neglected.[6]

It is important to note that the proposed mechanism can also be applied to the study of biofilms in which microbes utilize soluble electron transfer mediators. Step 3 would represent in this case the electron transfer from the cell to the soluble mediator and the diffusion of this species to the electrode interface.

Conduction along pili can also be considered by the model. In this case, step 3 would represent the electron transport along the conductive pili from the cells to the interfacial cytochromes.

Discharging the biofilm

As discussed above, during the discharge process the current can be separated into two contributions: oxidation of the reduced cytochromes and current production by cell metabolism. The mass balances of each species involved in the electron transfer processes have to be solved in order to derive the expression for the current transient. Only a basic analysis of the derivation of these equations is presented here and a detailed description can be found in the ESI†.

Interfacial cytochromes current. When discharge starts, the oxidation of cytochromes located at the electrode interface generates an enormous concentration gradient into the biofilm. This gradient drives steps 3 and 4 at a very high rate, producing an initial current that is much higher than the steady one (*e.g.* 88 A m^{-2} of initial current after 5 minutes at open circuit *versus* 4.4 A m^{-2} of steady current, in Fig. 3). This shows that, under some conditions, charge can be transferred in between cytochromes and to the electrode at a higher rate than that observed during normal operation.

Since interfacial cytochromes are the closest to the electrode, the oxidation pathway (step 4) obtained by applying a sufficiently high potential, will be faster than any other electron transfer process occurring in the biofilm during discharge. Thus, it can be considered that $k_{int} \gg k_{Omc}$. With this simplification, an estimation of the current generated by the re-oxidation of the reduced interfacial cytochromes (I_{Omc*}) can be easily found from the mass balance equation for this species (see ESI†):

$$I_{Omc*} = Fk_{int}Omc^*_{red0}\exp(-k_{int}t) \quad (1)$$

where Omc^*_{red0} is the number (in mol) of reduced interfacial cytochrome haems at the time of re-connection ($t = 0$). As it can be seen in eqn (1), the discharge current of the interfacial cytochromes (Omc^*) will follow an exponential decay that will depend on the value of the rate constant of the discharge (k_{int}) and the initial number (in mol) of reduced interfacial cytochrome haems (Omc^*_{red0}).

Matrix cytochromes current. Electron transfer from the cell interior to the outer mediators (step 2) includes transport steps

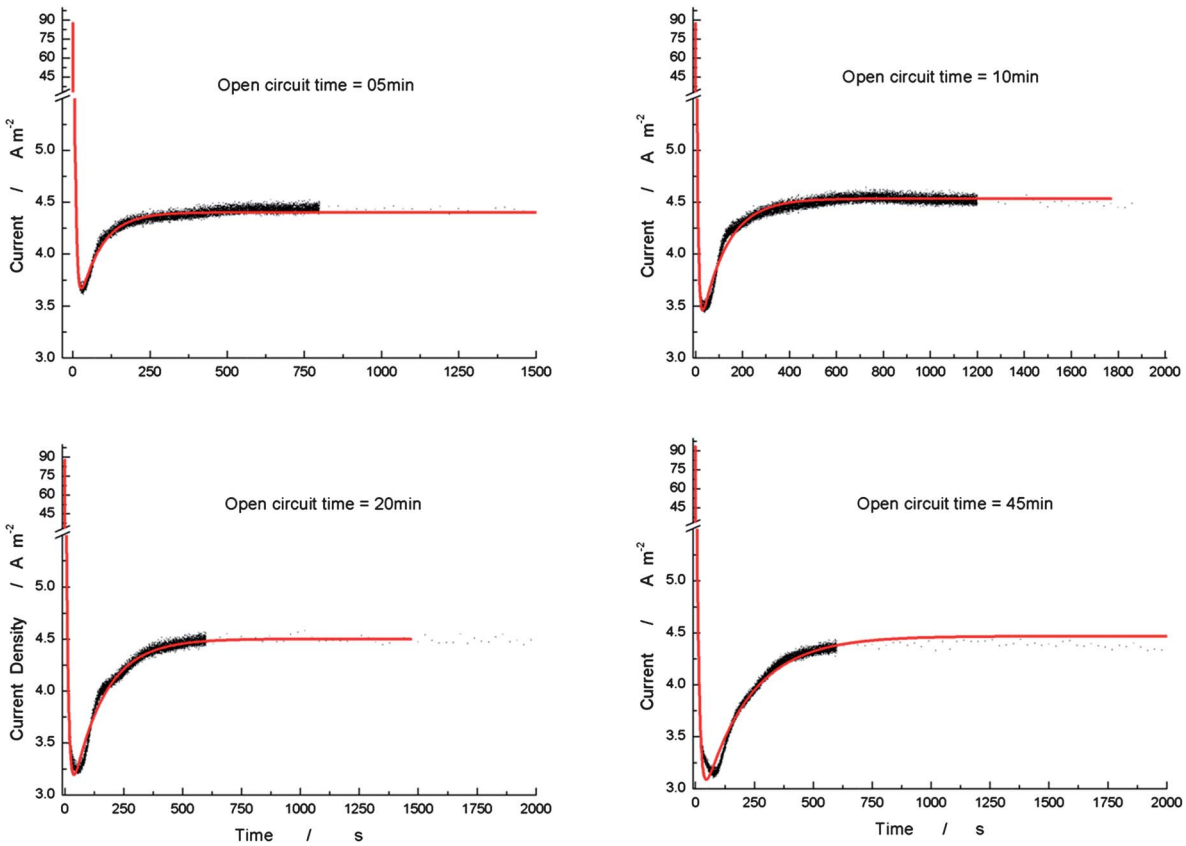

Fig. 3 Experimental (scatter) and modelled (red line) current densities for different open circuit times. Applied potential was 400 mV *vs.* SHE in all cases.

across membrane(s), facilitated by membrane conduits.[24] Unfortunately, the nature of this protein or its relative abundance compared to the internal or external cytochromes has not been yet determined for *G. sulfurreducens*. As hypothetically the cells synthesize only the necessary amount of proteins, the conduits number per cell will scale with the steady current. On the other hand, the external cytochromes form a conductive matrix that connects the whole biofilm to the electrode. It is considered here that the number of external cytochromes per cell is higher than the number of membrane conduits. Electrons can be thus transferred faster from the matrix of external cytochromes to the electrode than from the inside of the cell to the matrix. In the context of the proposed mechanism, this means that step 2 is slower than step 3. In addition, as interfacial cytochrome haems (Omc^*) are oxidized at a very high rate (see above), the number of reduced interfacial cytochrome haems can be considered virtually null ($Omc^*_{red} = 0$) during the re-oxidation of haems of cytochromes in the biofilm matrix (Omc). With these assumptions, the discharge current produced by re-oxidation of cytochromes (I_{Omc}) can be found from the simplified mass balance for this species (see ESI†):

$$I_{Omc} = Fk_{Omc}Omc^*_{tot}Omc_{red0}\exp(-k_{Omc}Omc^*_{tot}t) \quad (2)$$

where Omc_{red0} is the number of matrix cytochrome haems in the reduced form at the discharging process start time ($t = 0$), and Omc^*_{tot} is the total number (in mol) of interfacial cytochrome haems. The number of electron conduits is not directly considered in the mechanism, but the dependence of the current with this species is implicitly incorporated in the rate constant k_{mic}.

According to eqn (2), and as it was found for the interfacial cytochromes, the matrix cytochrome haems (Omc) re-oxidation follows an exponential decay. In this case, the time constant depends on the kinetics of the transfer between cytochrome haems, as well as on the total number of interfacial cytochrome haems (Omc^*_{tot}), because electrons stored in the matrix cytochromes have to be transferred to this species before being transferred to the electrode. Since it is considered that during the re-oxidation of matrix cytochromes all the interfacial cytochromes are already re-oxidized, the second order kinetic constant k_{Omc} is redefined as a pseudo-first order constant equal to $k_{Omc}Omc^*_{tot}$. The initial current depends on the initial number (in mol) of reduced cytochrome haems in the matrix (Omc_{red0}), and on the value of this pseudo-first order constant.

Acetate uptake and internal cytochromes current. As mentioned above, re-oxidation of internal cytochromes and acetate uptake process will also contribute to the current after electrode reconnection. Considering that step 3 is faster than steps 1 and 2 (see above), and that the initial number (in mol) of reduced cytochrome haems into the cells is Mic_{red0}, from mass balance in the reduced cells (see ESI†) it can be found that the current is given by:

$$\frac{I_{cells}}{F} = k_{mic}Omc_{tot}Mic_{red0}\exp\left[-(k_{mic}Omc_{tot}+k_{ac})t\right] + \frac{Mic_{tot}}{1/k_{ac}+1/k_{mic}Omc_{tot}}\left[1-\exp\left[-(k_{mic}Omc_{tot}+k_{ac})t\right]\right] \quad (3)$$

where Omc_{tot} is the total number of matrix cytochrome haems and Mic_{tot} represents the total haems in cell internal cytochromes. The first term in eqn (3) represents the re-oxidation of the cell internal cytochrome haems and the second the current produced by substrate uptake and subsequent electron transfer to extracytoplasmic cytochromes. As shown in this equation, when the discharge starts ($t = 0$) there is no activity of cell metabolism and the initial current is produced by the discharge of electrons stored in cell internal cytochromes. The rate of this last process decays in an exponential way as electrons are discharged, and simultaneously an exponential rise in metabolic activity occurs, yielding a final stabilization at the steady state current. The value of this current depends on the total number of internal cell cytochrome haems (Mic_{tot}) and the rate constants of steps 1 (k_{Ac}) and 2 ($k_{mic}Omc_{tot}$). No dependence with acetate concentration is predicted by the model, as it was considered that the current is independent of the substrate concentration when working at bulk concentrations higher than 5 mM. In the case of the lower substrate concentration, more complex reaction mechanisms incorporating, for example, Michaelis–Menten kinetics have to be solved.

Since it is considered that the internal cell cytochrome haems (Mic) start to get discharged once all the matrix cytochrome haems (Omc) had been oxidized, the second order kinetic constant k_{mic} is redefined as a pseudo-first order kinetic constant incorporating the total number of matrix cytochrome haems Omc_{tot}. The initial discharge current of the electrons in the internal cell cytochrome haems will depend on the value of this constant and on the initial number of reduced haems in the cell interior (Mic_{red0}).

Total current. The evolution of the current when the electrode is polarized again is the sum of the contributions of the re-oxidation of interfacial and matrix cytochrome haems (I_{Omc^*} and I_{Omc}, respectively), eqn (1) and (2), the re-oxidation of cell internal cytochrome haems and the uptake of substrate (I_{cells}), eqn (3):

$$\frac{I_{total}}{F} = \frac{I_{Omc^*}+I_{Omc}+I_{Cells}}{F} = k_{int}Omc^*_{red0}\exp(-k_{int}t) + k_{omc}Omc^*_{tot}Omc_{red0}\exp\left(-k_{omc}Omc^*_{tot}t\right) + k_{mic}Omc_{tot}Mic_{red0}\exp\left[-(k_{mic}Omc_{tot}+k_{ac})t\right] + \frac{Mic_{tot}}{1/k_{ac}+1/k_{mic}Omc_{tot}}\left[1-\exp\left[-(k_{mic}Omc_{tot}+k_{ac})t\right]\right] \quad (4)$$

Experimental

Biofilms of *Geobacter sulfurreducens* were grown in continuous mode in a 0.1 dm^3 stirred electrochemical cell using a 4 mm diameter graphite rod as the working electrode. The electrode surface was finished with 1000 grade silicon carbide paper and the geometric exposed area was 3 cm^2. The electrode potential was set at 0.4 V against the standard hydrogen electrode (SHE) using a Ag/AgCl—3 M NaCl electrode (RE-6 BASi, IN, USA) and a platinum wire as the reference and counter electrodes, respectively. A culture medium lacking electron acceptors containing 50 mM sodium bicarbonate solution and 20 mM acetate as the carbon source was prepared as described elsewhere.[25] The pH was kept constant at 7.3 by bubbling with a mixture of $N_2 : CO_2$ (80 : 20) through the solution. The gas mixture was filtered through a Variant C553120 oxygen filter to eliminate oxygen traces.

All the electrochemical assays were performed using an Autolab PGSTAT101 potentiostat controlled by Nova 1.6 dedicated software.

Biofilm thickness was measured by confocal microscopy after staining with acridine orange[26] (see ESI†). Chronopotentiometric (biofilm charge at open circuit) and chronoamperometric (biofilm discharge) experiments were alternately carried out on mature biofilms providing a steady state current density of approximately 4.5 A m^{-2}. The time at open circuit was progressively increased from 5 to 60 minutes to investigate the accumulation of charge. The discharge time, on the other hand, was always 1.5 h to ensure the stabilization of the biofilm at the steady state current and to avoid interference between experiments. Chronoamperometry data were fitted in OriginLab 8.0 with a five-parameter equation of the form:

$$I_{total} = A\exp(-k_1t) + B\exp(-k_2t) + C\exp(-k_3t) + D[1-\exp(-k_3t)] \quad (5)$$

which reproduces the functional form of the total current predicted from eqn (4). The parameters were:

$$A = Fk_{int}Omc^*_{red0} \quad B = Fk_{omc}Omc^*_{tot}Omc_{red0}$$

$$C = Fk_{mic}Omc_{tot}Mic_{red0} \quad D = F\frac{Mic_{tot}}{1/k_{ac}+1/k_{mic}Omc_{tot}}$$

$$k_1 = k_{int} \quad k_2 = k_{omc}Omc^*_{tot} \quad k_3 = k_{mic}Omc_{tot}+k_{ac}$$

F = Faraday constant

Parameter D was fixed at the stationary current value in all discharges to reduce the number of estimated parameters. Fitting was repeated with different initial parameter values to test convergence.

The rate constants of the proposed mechanism and the charge stored in interfacial, matrix and cell internal cytochrome haems were calculated from the parameters obtained from the non-linear regression analyses.

Rate constants of steps 3 and 4 correspond to the fitting parameters k_1 and k_2, respectively. Since the rate constants of steps 1 and 2 cannot be directly calculated from the fitting parameters, the calculation was made using parameter k_3 and the relative rate of each step, estimated from fluorescence analysis made by Esteve-Nuñez *et al.*[22] Once the kinetic parameters were obtained, the distribution of charge in the biofilm for the different times at open circuit was calculated from the fitting parameters. A detailed description of the calculations can be found in the ESI†.

An abiotic background experiment in which current transients were measured in the same media for an electrode without biofilm is shown in the ESI†. In this case, the open circuit time was 20 minutes and discharge potential was varied from −0.2 to 0.4 V (SHE).

Model results and discussion

The discharge current densities and the corresponding fits for 5, 10, 20 and 45 minutes at open circuit are shown in Fig. 3. As current produced by discharge of the double layer (see abiotic background experiments in the ESI†) was orders of magnitude lower than the current produced by the biofilms, its contribution to current was neglected during calculations.

The fitting results obtained from the fit to eqn (5) are in very good agreement with experimental data up to a disconnection time of approximately 45 min. From this time on, the decay kinetics of the measured current close to the minimum current is clearly slower than that predicted by the model, suggesting that charge transfer processes not considered in the model might arise after a prolonged disconnection (time > 45 min).

In accordance with the initial assumptions the calculated electron transfer rate between interfacial cytochromes and the electrode (step 4) is very high ($k_{int} = 13 \pm 1\ s^{-1}$) agreeing with the order of the typical heterogeneous oxidation rate of cytochromes at modified electrodes[27,28] and with previous results[29] that indicate the reversibility of the cytochrome–electrode interaction. Electron transfer from cytochromes present in the matrix to interfacial cytochromes (step 3), on the other hand, is slower by two orders of magnitude ($k_{Omc}.Omc^{*}_{tot} = 0.12 \pm 0.03\ s^{-1}$) as expected from a process including multiple intermolecular (cytochrome-to-cytochrome) steps for the transport of electrons. The electron transport through the matrix has been highlighted by Strycharz *et al.* as the step that limits the overall electron transport process,[30] implicitly indicating its relative slow rate as compared to interfacial ET processes. However, this conclusion mainly derives from voltammetric measurements performed under acetate depletion, thus excluding metabolic constraints. In the presence of acetate, the rate of electron transport across the matrix does not appear to be the limiting step in current production. The combined rate of acetate oxidation by the cells (step 1) and electron transfer step from the internal to exocytoplasmic cytochromes (step 2) appears to be much slower ($k_{ac} + k_{mic}Omc_{tot} = 0.01 \pm 0.005\ s^{-1}$), which indicates that the limitation for current production can be in either of these two steps. From the fluorescence analysis by Esteve-Nuñez *et al.*,[22] it could be estimated that electron transfer to exocytoplasmic cytochromes (step 2) is approximately 11 times faster than microbial uptake of acetate and transfer to internal cytochromes (step 1) (see ESI†), yielding $k_{ac} = 0.0008\ s^{-1}$ and $k_{mic}Omc_{tot} = 0.0092\ s^{-1}$. This analysis points at the processes involved in electron transfer from acetate uptake to internal cytochromes as the main limitation for current production, in agreement with the conclusion by Richter *et al.* (2009) based on the analysis of *G. sulfurreducens* biofilms by cyclic voltammetry.[6]

The amount of charge stored in the cells, the matrix and the interfacial cytochromes for all disconnection times was also calculated. Interestingly, the accumulation of charge in the interfacial cytochromes followed an inverse relation with the open circuit potential (OCP) (Fig. 4). This strongly supports the previous assumption that the OCP is an indicator of the redox state of interfacial cytochromes,[17] agreeing also with the recently shown relation between the electrode potential and concentration of interfacial cytochromes in the reduced form.[29] It also indicates that the charge accumulation at the biofilm–electrode interface might be a plausible explanation for the non-linear overpotential obtained in microbial fuel cells[31,32] when the current interrupt technique is used. For times shorter than 20 minutes, the experimental OCP and the calculated interfacial charge remain almost constant. For longer times, an evolution of the OCP to more negative values is observed. This is explained by the model as a progressive increase of the interfacial charge. It is interesting to note that OCP values obtained at long disconnection times are more positive than the negative end of the redox range of both OmcZ and OmcS, external cytochromes known to compose the external matrix of *Geobacter* biofilms.[33,34] Comparing the obtained potential for large open circuit times (Fig. 4) with SERR spectroscopy results that show the change of interfacial cytochrome haems redox state with the potential of the electrode[29] suggests that bacteria are not able to reduce interfacial cytochrome haems beyond about 90%. The function of the remaining 10% of haem groups is still unknown.

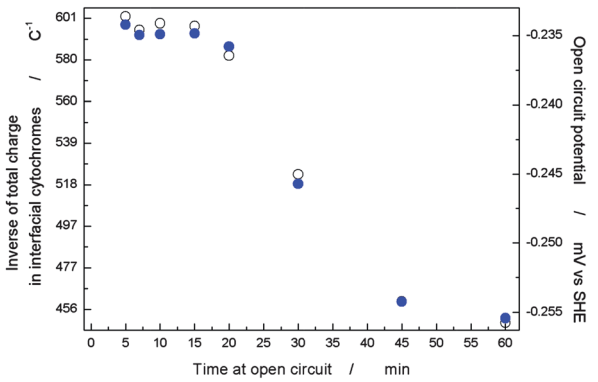

Fig. 4 Inverse of charge stored in interfacial cytochromes (empty circles) and OCP value *vs.* SHE (blue circles) against time at open circuit.

In agreement with previous data,[35] an interfacial charge density on the order of 5–7 × 10^{-9} mol of electrons per cm^2 of electrode area can be estimated from results in Fig. 4.

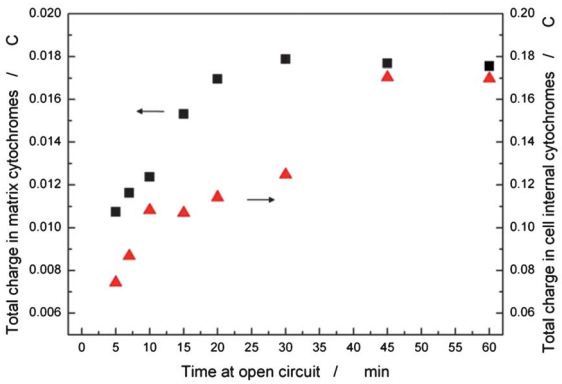

Fig. 5 Charge stored in matrix (black squares) and cell internal (red triangles) cytochromes against open circuit time.

Considering recently reported mean diameters of approximately 8.5 nm for multi-haem cytochromes,[24,36] the maximum packing for a monolayer of spherical proteins yields about 2.7×10^{-12} mol of proteins per cm^2. A simple calculation using this value and the estimated charge density calculated from the model (see above) and the reduction of 90% of the haems (*e.g.* 7 of 8 in OmcZ) indicates that the estimated interfacial charge is not located in a single layer,[35] but should be distributed over 300–400 protein layers. This calculation indicates that interfacial cytochromes have to be considered as those able to rapidly exchange electrons with the electrode, though not necessarily in direct contact with it. In this regard, it is important to note that the contribution to the measured current of the oxidation of only the cytochromes in direct contact with the electrode would be too small to be experimentally quantified, *e.g.*: a monolayer with a packing of 2.7×10^{-12} mol of proteins per cm^2 discharging at a rate equal to the initial current shown in Fig. 3 (88 A m^{-2}) would take only 0.2 milliseconds to discharge completely.

The charge stored in the matrix cytochromes grows up fast during the first 20 minutes at open circuit (Fig. 5), reaching later a steady value. As charge is accumulated in the matrix, the reduction of lower potential haems in interfacial cytochromes may be forced, which could explain the change on the OCP to more negative potentials observed beyond 20 minutes.

The amount of charge stored in the matrix cytochromes is one-fold higher than the interfacial charge (Fig. 4 and 5). Considering *G. sulfurreducens* cells of 0.5 μm in diameter and 2 μm in length,[37] 2.1×10^{10} cells can be estimated to compose the biofilm with a typical cell coverage of 20%[38] and a biofilm total volume of 0.041 cm^3 calculated from thickness measurements by confocal microscopy (see the ESI†). In this scenario, the matrix charge estimated by the model (Fig. 5) represents approximately 5×10^6 electrons in external cytochromes per cell, suggesting that each bacterial cell would be ideally covered by about 8–9 layers of cytochromes of 8.5×10^{-3} μm [24,36] in size.

On the other hand, maximum charge stored in the cell internal cytochromes is 0.17 C (Fig. 5). According to the estimated number of cells in the biofilm, the number of electrons stored per cell in internal cytochromes is 5.4×10^7, which is in the order of the storage capacity reported for suspended cells.[22]

Charge storage in cytochromes allows suspended cells of *G. sulfurreducens* maintaining basic energy dependent processes for approximately 8 minutes.[22] This time has been found to be longer in electricity-producing biofilms that are able to overcome much longer times of disconnection without losing activity. According to the presented results, the explanation for this observation is not found on the use of external cytochromes as an additional sink because, notably, charge storage in cell external cytochromes represents only a minor fraction (10%) of that in the cell interior (Fig. 5). The reasons behind the superior ability of biofilm cells to survive in the absence of an electron acceptor are thus still unknown.

Conclusions

A novel approach to study electron transfer mechanisms in electricity producing biofilms has been presented. It is based on modeling the transient current profile that is obtained after leaving the biofilm at open circuit for a period of time and then reconnecting the electrode. The model allows the numerical estimation of rate constants for the kinetics of the steps involved in electron transport from the substrate to the electrode and of the stored charge distribution into the biofilm, distinguishing between periplasmic (cell internal), matrix and interfacial cytochromes. To our knowledge, it represents the first experimental approach for the determination of these biofilm parameters.

According to the presented results, electron transfer from acetate to cell internal cytochromes is the overall limitation to the catalytic current production. Future effort for achieving more efficient current generation with electrogenic microorganisms as *G. sulfurreducens* should thus be aimed at improving the electron production rate of the cells, *e.g.* by searching more active electrogenic species in natural environments, modifying cells using genetic engineering or by developing anodes that support an increased number of cells per unit area.

It is also concluded that charge is stored mainly in the periplasmic cytochromes, *i.e.* at the cell interior, indicating that the main function of cytochromes in the biofilm matrix would not be sustaining cell activity in the absence of external electronic acceptors. Instead, a role in electron transport through the biofilm matrix is supported by data presented here.

The novel experimental approach presented here will hopefully help to achieve a deeper understanding of electron transport in electricity-producing biofilms.

Acknowledgements

We are grateful to constructive discussions with Professor David Schiffrin. We would like to thank the reviewers for the thoughtful observations that improved the quality of our work. The technical assistance of Juan Assarou and José Kochur from INTEMA is greatly acknowledged. The work was supported by the European Union through the BacWire FP7 Collaboration project (contract #: NMP4-SL-2009-229337). PSB, GS and LR are doctoral fellows from CONICET, Argentina.

References

1 D. R. Lovley, *Geobiology*, 2008, **6**, 225–231.
2 D. R. Lovley and K. P. Nevin, *Curr. Opin. Biotechnol.*, 2011, **22**, 441–8.
3 U. Schröder, *Phys. Chem. Chem. Phys.*, 2007, **9**, 2619–2629.
4 O. Bretschger, Y. Gorby and K. H. Nealson, in *Bioelectrochemical Systems: From Extracellular Electron Transfer to Biotechnological Application*, ed. K. Rabaey, L. Angenent, U. Schröder and J. Keller, IWA Publishing, 2010, ch. 7, pp. 81–100.
5 C. I. Torres, A. K. Marcus, H.-S. Lee, P. Parameswaran, R. Krajmalnik-Brown and B. E. Rittmann, *FEMS Microbiol. Rev.*, 2010, **34**, 3–17.
6 H. Richter, K. P. Nevin, H. Jia, D. A. Lowy, D. R. Lovley and L. M. Tender, *Energy Environ. Sci.*, 2009, **2**, 506–516.
7 E. Marsili, J. B. Rollefson, D. B. Baron, R. M. Hozalski and D. R. Bond, *Appl. Environ. Microbiol.*, 2008, **74**, 7329–7337.
8 J. P. Busalmen, A. Esteve-Núñez, A. Berná and J. M. Feliu, *Angew. Chem., Int. Ed.*, 2008, **47**, 4874–4877.
9 T. Mehta, M. V. Coppi, S. E. Childers and D. R. Lovley, *Appl. Environ. Microbiol.*, 2005, **71**, 8634–8641.
10 D. R. Lovley, *Curr. Opin. Biotechnol.*, 2008, **19**, 564–571.
11 A. Kato Marcus, C. I. Torres and B. E. Rittmann, *Biotechnol. Bioeng.*, 2007, **98**, 1171–1182.
12 J. B. Rollefson, C. S. Stephen, M. Tien and D. R. Bond, *J. Bacteriol.*, 2011, **193**, 1023–1033.
13 N. S. Malvankar, M. Vargas, K. P. Nevin, A. E. Franks, C. Leang, B.-C. Kim, K. Inoue, T. Mester, S. F. Covalla, J. P. Johnson,

V. M. Rotello, M. T. Tuominen and D. R. Lovley, *Nat. Nanotechnol.*, 2011, **6**, 573–579.
14 G. Reguera, K. D. McCarthy, T. Mehta, J. S. Nicoll, M. T. Tuominen and D. R. Lovley, *Nature*, 2005, **435**, 1098–1101.
15 D. R. Lovley, T. Ueki, T. Zhang, N. S. Malvankar, P. M. Shrestha, K. A. Flanagan, M. Aklujkar, J. E. Butler, L. Giloteaux, A.-E. Rotaru, D. E. Holmes, A. E. Franks, R. Orellana, C. Risso and K. P. Nevin, in *Advances in Microbial Physiology*, ed. K. P. Robert, Academic Press, 2011, vol. 59, pp. 1–100.
16 D. R. Lovley, *Energy Environ. Sci.*, 2011, **4**, 4896–4906.
17 G. D. Schrott, P. S. Bonanni, L. Robuschi, A. Esteve-Nuñez and J. P. Busalmen, *Electrochim. Acta*, 2011, **56**, 10791–10795.
18 S. M. Strycharz-Glaven, R. M. Snider, A. Guiseppi-Elie and L. M. Tender, *Energy Environ. Sci.*, 2011, **4**, 4366–4379.
19 C. s. I. Torres, A. K. Marcus, P. Parameswaran and B. E. Rittmann, *Environ. Sci. Technol.*, 2008, **42**, 6593–6597.
20 A. K. Marcus, C. I. Torres and B. E. Rittmann, *Biotechnol. Bioeng.*, 2007, **98**, 1171–1182.
21 S. M. Strycharz, A. P. Malanoski, R. M. Snider, H. Yi, D. R. Lovley and L. M. Tender, *Energy Environ. Sci.*, 2011, 896–913.
22 A. Esteve-Nunez, J. Sosnik, P. Visconti and D. R. Lovley, *Environ. Microbiol.*, 2008, **10**, 497–505.
23 A. J. Bard and L. R. Faulkner, *Electrochemical Methods: Fundamentals and Applications*, John Wiley & Sons, 2001.
24 T. A. Clarke, M. J. Edwards, A. J. Gates, A. Hall, G. F. White, J. Bradley, C. L. Reardon, L. Shi, A. S. Beliaev, M. J. Marshall, Z. Wang, N. J. Watmough, J. K. Fredrickson, J. M. Zachara, J. N. Butt and D. J. Richardson, *Proc. Natl. Acad. Sci. U. S. A.*, 2011, **108**, 9384–9389.
25 A. Esteve-Nunez, M. Rothermich, M. Sharma and D. Lovley, *Environ. Microbiol.*, 2005, **7**, 641–648.
26 A. Jain, G. Gazzola, A. Panzera, M. Zanoni and E. Marsili, *Electrochim. Acta*, 2011, **56**, 10776–10785.
27 W. J. Albery, M. J. Eddowes, H. A. O. Hill and A. R. Hillman, *J. Am. Chem. Soc.*, 1981, **103**, 3904–3910.
28 Z. Zhang, A.-E. F. Nassar, Z. Lu, J. B. Schenkman and J. F. Rusling, *J. Chem. Soc., Faraday Trans.*, 1997, **93**, 1769–1774.
29 D. Millo, F. Harnisch, S. A. Patil, H. K. Ly, U. Schröder and P. Hildebrandt, *Angew. Chem., Int. Ed.*, 2011, **50**, 2625–2627.
30 S. M. Strycharz, R. H. Glaven, M. V. Coppi, S. M. Gannon, L. A. Perpetua, A. Liu, K. P. Nevin and D. R. Lovley, *Bioelectrochemistry*, 2011, **80**, 142–150.
31 F. Zhao, R. C. T. Slade and J. R. Varcoe, *Chem. Soc. Rev.*, 2009, 1926–1939.
32 B. E. Logan, B. Hamelers, R. Rozendal, U. Schroder, J. Keller, S. Freguia, P. Aelterman, W. Verstraete and K. Rabaey, *Environ. Sci. Technol.*, 2006, **40**, 5181–5192.
33 K. Inoue, C. Leang, A. E. Franks, T. L. Woodard, K. P. Nevin and D. R. Lovley, *Environ. Microbiol. Rep.*, 2011, **3**, 211–217.
34 C. Leang, X. Qian, T. Mester and D. R. Lovley, *Appl. Environ. Microbiol.*, 2010, **76**, 4080–4084.
35 E. LaBelle and D. R. Bond, in *Bioelectrochemical Systems: From Extracellular Electron Transfer to Biotechnological Application*, ed. K. Rabaey, L. Angenent, U. Schröder and J. Keller, IWA Publishing, 2010, ch. 8, pp. 135–152.
36 A. Johs, L. Shi, T. Droubay, J. F. Ankner and L. Liang, *Biophys. J.*, 2010, **98**, 3035–3043.
37 F. Caccavo, Jr, D. J. Lonergan, D. R. Lovley, M. Davis, J. F. Stolz and M. J. McInerney, *Appl. Environ. Microbiol.*, 1994, **60**, 3752–3759.
38 J. P. Busalmen and S. R. de Sánchez, *Appl. Environ. Microbiol.*, 2001, **67**, 3188–3194.